

# Measured and simulated electric, magnetic, and thermal field distributions of a patch antenna operating at high power

Ronald M. Reano\*, Werner Thiel, and John F. Whitaker

Electrical Engineering and Computer Science Dept., University of Michigan, Ann Arbor, 1301 Beal Ave., Ann Arbor, Michigan 48109-2122, email: reanorm@umich.edu

Linda P. B. Katehi

School of Engineering, Purdue University, 1280 Engineering Administration, West Lafayette, Indiana 47907-1280

**Abstract:** Electric, magnetic, and thermal field distributions in the near field of a microstrip patch antenna operating at high RF power are experimentally determined. Electro-optic sampling is used to obtain the electric field distribution, magneto-optic sampling provides the magnetic field distribution, and semiconductor bandgap thermometry is used to obtain the thermal field. Measurements are compared with simulations and are found to be in good agreement. From the measurements, it is concluded that dielectric loss, in the substrate of the structure, is the dominant loss mechanism in the antenna.

## 1. Introduction

Field mapping of electric, magnetic, and thermal field distributions in the near field of high-power microwave/millimeter-wave circuits and radiating structures provides information useful for diagnostic purposes, prototype design, and an overall understanding of operational behavior. Methods to measure electric fields have included coaxial and dipole antenna-based probes, modulated scattering probes, scanning-force-microscopy-based probes, and electro-optic-based probes [1]-[4]. Techniques to measure magnetic fields have utilized conducting loop-based probes, as well as magneto-optic based probes [5]-[7]. Yang *et al* have obtained two-dimensional electric field maps of a 4 GHz patch antenna operating at low RF power using electro-optic sampling [8]. Yamazaki *et al* have obtained two-dimensional magnetic field maps of low-frequency coupled lines using a magneto-optic based probe [9]. To observe thermal effects, methods include the use of thermal cameras, infrared microscopes, thermocouples, and thermistors. In addition, it has been shown that the temperature sensitivity of the bandgap of gallium arsenide can be used to study temperature variations in active microwave circuits [10]. In this paper, electro-optic sampling, magneto-optic sampling, and semiconductor bandgap thermometry are used together to characterize an X-band patch antenna operating at high RF power (8 watts RF). Each technique is shown to provide complementary information yielding a thorough picture of the electromagnetic behavior and associated thermal effects.

## 2. Measurement Description

Full details of the experimental techniques utilized in this work can be found in references 10 and 11. Briefly, point measurement probes are raster scanned in order to produce two-dimensional maps of the desired fields. To measure electric fields, a GaAs electro-optic probe with physical dimensions of 500  $\mu\text{m}$  x 500  $\mu\text{m}$  x 200  $\mu\text{m}$  is employed. Due to the Pockels effect, an optical beam propagating through the electro-optic material exhibits a change in its polarization state when the material is in the presence of an externally applied electric field of low frequency compared with the optical field. The change in polarization state can be made to result in an amplitude modulation of the optical beam that is proportional to the intensity of the applied electric field.

To measure magnetic fields, a probe based on Faraday-effect polarization sensitivity is used. The probe consists of a circular cylinder of terbium gallium garnet (2-mm diameter, 2-mm length). An optical beam passing through the material experiences circular birefringence in response to an externally applied magnetic field. The rotation of the polarization state of the beam can be made to result in an amplitude modulation of the optical beam that is proportional to the intensity of the applied magnetic field.

For temperature measurements, the optical absorption upon propagation through the probe is monitored. Due to the temperature dependence of the bandgap of the semiconductor, the optical transmissivity through the probe is modulated by variations in probe temperature. A field-map is obtainable once the temperature profile reaches steady state.

### 3. Results and Discussion

For the current experiment, a patch antenna was fabricated on copper-metallized RT/duroid 6006 ( $\epsilon_r = 6.15$ ,  $\tan \delta = 0.0027$ ,  $h = 25$  mil). The antenna is fed with a recessed microstrip in conjunction with a quarter-wave matching section and was operated at resonance (10.403 GHz) with 8 watts of RF input power. The ground plane of the antenna was mounted on a metallic base in order to allow for heat-sinking. Due to the symmetry of the antenna, it was only necessary to scan one-half of the desired image.

The measured and simulated  $z$ -component of the electric field is shown in Fig. 1 at a height of 0.5 mm above the surface. Simulation results were obtained using a finite-element-method solver [12]. The measured and simulated results are in good agreement and show that the mode in the dielectric beneath the patch resembles the  $TM_{10}$ -mode to  $z$  as described in the cavity model [13].

Measured and simulated results of the  $y$ -component of the magnetic field at a height of 1.5 mm are shown in Fig. 2. Simulation results were once again obtained using finite-element-method simulations [12]. In the limit of zero height above the surface and infinite metal conductivity, the  $y$ -component of the magnetic field theoretically limits to the surface current on the metal. In the measured field map, the regions of high magnetic field are consistent with the presence of large currents, on the top metallization of the patch, along the non-radiating edges.

The measured temperature profile at a height of 0.5 mm above the patch antenna is shown in Fig. 3. Once the RF power was turned on, the temperature reached steady-state after approximately one minute, thereby allowing for the imaging of the temperature distribution. In the measurement, hot spots are observed at the top edge of the antenna and at the bottom edge in the vicinity of the microstrip feed where the temperature peaks at forty degrees. This is approximately 20 °C above the ambient laboratory temperature. The temperature distribution is seen to fall away rapidly with lateral distance from the antenna.

To gain insight into these results, the measured thermal image was compared with simulations. In order to obtain the simulated temperature distribution of the patch antenna, a finite-difference-time-domain technique was applied to both the electromagnetic problem and to the thermal problem. Details of the numerical technique can be found in reference 14. In a preceding electromagnetic simulation, the dissipated power in the conductor and in the lossy substrate was calculated. For an accurate modeling of the skin effect in the conductor, an effective complex conductivity was introduced [15]. The resulting dissipated power was the basis for a subsequent heat analysis where a forward-time centered-space (FTCS) scheme was applied to the conductive heat equation [16], [17]. In this approach, thermal radiation and convection in the computational domain were not taken into account. The domain was terminated by boundary conditions that modeled the heat sink underneath the substrate and the convection on the boundary above the patch.

The measured and simulated temperature profiles are in good agreement except in two areas. The first is the hot spot at the tip of the patch, which shows up in the measurement but not in the simulation. The second is the difference in peak temperature. The first difference between the measured and simulated temperature profiles can be attributed to the surface contact between the heat sink and the patch antenna ground plane. Experimentally, this was accomplished via double-sided tape, which was not modeled in the simulation. The small air gap allowed for less than ideal conduction into the heat sink, thereby providing for a greater proportion of heat flow in the direction opposite to the heat sink, ultimately changing the temperature distribution above the patch. The difference in peak temperatures can be attributed to the lack of modeling convection in the computational domain. In the absence of convection, the simulation predicts a higher temperature

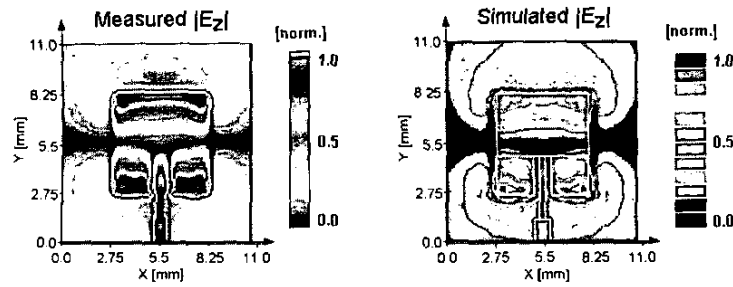


Fig. 1. Measured and simulated magnitude of the z-component (normal) of the electric field at a height of 0.5 mm above the surface.

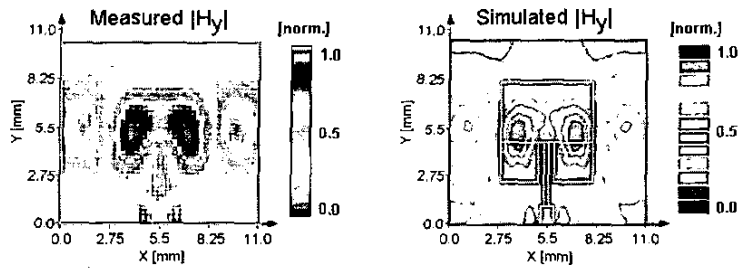


Fig. 2. Measured and simulated magnitude of the y-component (tangential) of the magnetic field at a height of 1.5 mm above the surface.

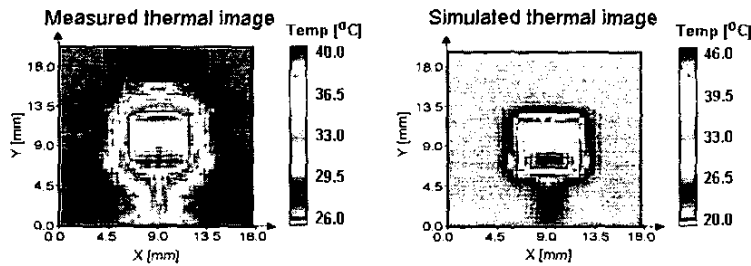


Fig. 3. Measured and simulated temperature distribution at a height of 0.5 mm above the surface.

than expected in measurements because the presence of convection introduces air-flow across the surface. Other than these two exceptions, the thermal measurement is in good agreement with the simulation.

It is interesting to note that the two hot spots observed in the measured temperature distribution correlate in location with the maxima of the electric field mode supported in the dielectric between the patch and the ground plane. This is contrary to an initial expectation that the temperature distribution should map according to the location of the currents on the patch. In the structure, however, there are

two primary loss mechanisms: (1) loss in the metal due to the finite conductivity, and (2) loss in the dielectric due to conductivity loss and dielectric damping [18]. Since the temperature measurements show that the hot spots correlate with the mode in the dielectric where the electric field peaks and not with the current distribution where the magnetic field peaks, it is concluded that dielectric loss dominates the temperature profile.

#### 4. Conclusion

Measurements and simulations of electric, magnetic, and thermal field distributions of an X-band patch antenna operating at high RF power are presented. Field mapping of the electric field yields information regarding the resonant mode whereas magnetic field data provides insight into the location of large currents. The temperature profile, when compared against electric and magnetic field distributions, conveys the mechanism behind the losses. When used together, these techniques allow for a thorough characterization of high-power microwave/millimeter wave circuits and radiating structures.

#### Acknowledgements

This work has been sponsored by the MURI program on "Spatial and Quasi-Optical Power Combining" monitored by the Army Research Office Grant No. DAAG 55-97-0132 under subcontract to Clemson University.

#### References

- [1] Y. J. Gao and I. Wolff, "Miniature electric near-field probes for measuring 3-D fields in planar microwave circuits," *IEEE Trans. Microwave Theory Tech.*, vol. 46, pp. 907-913, July 1998.
- [2] T. P. Budka and G. M. Rebeiz, "A microwave circuit electric field imager," *1995 IEEE MTT-S Int. Microwave Symp. Dig.*, vol. 3, pp. 1139-1142, May 1995.
- [3] C. Bohm, C. Roths, and E. Kubalek, "Contactless electric characterization of MMIC's by device internal electrical sampling scanning-force-microscopy," *1994 IEEE MTT-S Int. Microwave Symp. Dig.*, vol. 3, pp. 1605-1608, May 1994.
- [4] M. Shinagawa and T. Nagatsuma, "Electro-optic sampling using an external GaAs probe tip," *Electron. Lett.*, vol. 26, pp. 1341-1343, Aug. 1990.
- [5] Y. J. Gao and I. Wolff, "A new miniature magnetic field probe for measuring three-dimensional fields in planar high-frequency circuits," *IEEE Trans. Microwave Theory Tech.*, vol. 44, pp. 911-918, June 1996.
- [6] S. Wakana, T. Ohara, M. Abe, E. Yamazaki, M. Kishi, and M. Tsuchiya, "Fiber-edge electrooptic/magneto-optic probe for spectral-domain analysis of electromagnetic field," *IEEE Trans. Microwave Theory and Tech.*, vol. MTT-48, pp. 2611-2616, Dec. 2000.
- [7] P. H. Harms, J. G. Maloney, M. P. Kesler, E. J. Kuster, G. S. Smith, "A System for Unobtrusive Measurement of Surface Currents," *IEEE Trans. Antennas Propagat.*, vol. 49, pp. 174-184, Feb 2001.
- [8] K. Yang, G. David, J. G. Yook, I. Papapolymerou, L. P. B. Katehi, J. F. Whitaker, "Electro-optic mapping and finite-element modeling of the near-field pattern of a microstrip patch antenna," *IEEE Trans. Microwave Theory Tech.*, vol. 48, pp. 288-294, Feb 2000.
- [9] E. Yamazaki, S. Wakana, M. Kishi, M. Iwanami, S. Hoshino, and M. Tsuchiya, "Three-dimensional magneto-optic near-field mapping over 10-50 micron-scale line and space circuit patterns," *2001 IEEE LEOS Conf. Proceedings*, vol. 1, pp. 318-319, Nov. 2001.
- [10] R. M. Reano, K. Yang, L. P. B. Katehi, and J. F. Whitaker, "Simultaneous measurements of electric and thermal fields utilizing an electro-optic semiconductor probe," *IEEE Trans. Microwave Theory Tech.*, vol. 49, pp. 2523-2531, Dec. 2001.
- [11] R. M. Reano, J. F. Whitaker, L. P. B. Katehi, "Field-tunable probe for combined electric and magnetic field measurements," *to appear in 2002 IEEE MTT-S Int. Microwave Symp. Dig.*, Jun. 2002.
- [12] *Ansoft HFSS Release 8*, Pittsburgh, PA, 2001.
- [13] K. R. Carver and J. W. Mink, "Microstrip Antenna Technology," *IEEE Trans. Antennas Propagat.*, vol. AP-29, pp. 2-24, Jan. 1981.
- [14] W. Thiel, K. Tornquist, R. Reano and L.P.B. Katehi, "A Study of Thermal Effects in RF-MEM-Switches using a Time Domain Approach", *to appear in 2002 IEEE MTT-S Int. Microwave Symp. Dig.*, Jun. 2002.
- [15] W. Thiel, "A Surface Impedance Approach for Modeling Transmission Line Losses in FDTD", *IEEE Microwave Guided Wave Lett.*, vol. 10, no. 3, pp. 89-91, March 2000.
- [16] J.W. Thomas, *Numerical Partial Differential Equations, Finite Difference Methods*, New York: Springer, 1995.
- [17] A.J. Chapman, *Fundamentals of Heating Transfer*, New York: McMillan Publishing Comp., 1987.
- [18] D. M. Pozar, *Microwave Engineering, 2<sup>nd</sup> Ed.*, New York: John Wiley and Sons, Inc., 1998.